-1

Au: Return with last batch of Page Proofs

ATMOSPHERIC REMOTE SENSING BY MICROWAVE RADIOMETRY

Atmospheric Remote Sensing by Microwave Radiometry.

Master Set

Ed. Cannot break H.T. or Title per msp. Should we match line breaks on both?

WORK12 A6416$AFMT

WILEY SERIES IN REMOTE SENSING

Jin Au Kong, Editor

Tsang, Kong, and Shin . THEORY OF MICROWAVE REMOTE SENSING

Herd • REMOTE SENSING: METHODS AND APPLICATIONS

Elachi • INTRODUCTION TO THE PHYSICS AND TECHNIQUES OF REMOTE SENSING

Szekielda • SATELLITE MONITORING OF THE EARTH

Maffett • TOPICS FOR A STATISTICAL DESCRIPTION OF RADAR CROSS SECTION

Asrar . THEORY AND APPLICATIONS OF OPTICAL REMOTE SENSING

Curlander and McDonough • SYNTHETIC APERTURE RADAR: SYSTEMS AND SIGNAL PROCESSING

Haykin • ADAPTIVE RADAR DETECTION AND ESTIMATION

Janssen • ATMOSPHERIC REMOTE SENSING BY MICROWAVE RADIOMETRY

ATMOSPHERIC REMOTE SENSING BY MICROWAVE RADIOMETRY

Edited by
Michael A. Janssen

A WILEY-INTERSCIENCE PUBLICATION
JOHN WILEY & SONS, INC.
New York • Chichester • Brisbane • Toronto • Singapore

WORK 12 A64 16$AFMT

This text is primed on acid-free paper.

Library of Congress Cataloging in Publication Data:

Janssen, Michael A., 1937-

Atmospheric rermote sensing by microwave radiometry / Michael A. Janssen.

p. cm. – (Wiley series in remote sensing)

"A Wiley -Interscience publication. "

Includes bibliographical references and index.

ISBN O-471 -62891-3 (alk. paper)

1. Atprosphere-Remote sensing. 2. Atmospheric radiation—Measurement. 3. Microwave remote sensing. 1. Title. 11. Series.

QC87 1.J26 1992-93

551.5'028--dc20 92-12794

CIP

Printed in the United States of America,

1 0 9 8 7 6 - 5 4 3 2 1

To **Glenys, Sandie,** *and Liza*

CONTRIBUTORS

R. TODD CLANCY Laboratory for Astrophysics and Space Physics, University of Colorado at Boulder, Boulder, CO .

GUNNAR ELGERED Onsala Space Observatory, Chalmers University of Technology, Onsala, Sweden

A. J. GASIEWSKI School of Electrical Engineering, Georgia Institute of Technology, Atlanta, GA . . . .

NORMAN C. GRODY National Environmental Satellite Data and Information Service, National Oceanic and Atmospheric Administration, Camp Springs, MD

SAMUEL GULKIS ..-Jet Propulsion Laboratory, California Institute of Technology, Pasadena, CA - . .

MICHAEL A. JANSSEN Jet Propulsion Laboratory, California Institute of Technology, Pasadena CA

DUANE O. MUHLEMAN Division of Geological and Planetary Sciences. California Institute of Technology, Pasadena, CA

PHILLIP W. ROSENKRANTZ "Research Laboratory of Electronics, Massachusetts Institute of Technology, Cambridge, MA

J. W. WATERS Jet Propulsion Laboratory, California Institute of Technology, Pasadena, CA'

ED R. WESTWATER Wave Propagation Laboratory, Environmental Research Laboratory, National Oceanic and Atmospheric Administration, Boulder, CO

CONTENTS

Note: This is right but text is wrong (2.2.4)

Ed: delete "Transf ?"

Note these are subheads of 4.1.3 Incorrect pages

Insert (A)

(A) Use of Radar Measurements of Tropopause Height to Improve Radiometric Temperature Retrievals

WORK12 A6416$AFMT

605-722

PREFACE

The Earth's atmosphere is a puzzle and a concern. Its unpredictable weather has always been a force to be reckoned with, but until recent times, our trust was implicit in the robustness of the atmospheric system as the foundation of our biosphere. Now we are not so sure. Far from being robust, this system is probably better described as a balance among a number of natural forces, which we barely understand and our concern is deepened when we consider the threat to this balance from our burgeoning civilization and its effluents. What, for example, are the chlorofluorocarbons doing to the ozone layer, and how significantly and on what time scales will the increasing $C0_2$ production change the climate? There will be no answers to such questions without a strong and steady program of research to understand fundamental atmospheric processes. Essential to this is the gathering of basic data such as temperature, pressure, wind, and the distribution of water vapor, clouds, and other active constituents. Such data enable us to test existing models for the atmosphere's energy balance, the depletion of the ozone layer, the hydrological cycle, climate trends, and other aspects of the atmospheric system that are of vital interest to us, and to formulate new and better models to guide us in the future. Remote sensing is central to this effort because it is the only way we can obtain full spatial and temporal perspective needed to understand atmospheric processes. The strong conclusion is that the need for remote sensing will continue, and grow.

Microwaves, which we take as a generic term to include the centimeter, millimeter, and submillimeter regions of the spectrum, play a special role in the remote sensing of atmospheres. Microwave techniques bring a mixture of capabilities that complement remote-sensing methods used in other spectral regions. Microwaves penetrate clouds. for example, and provide an all-weather measurement capability as well as the only direct means for the determination of cloud water content. The coherent detection technique that characterizes microwave receivers allows the emission lines of atmospheric constituents to be examined with arbitrarily high-frequency resolution, Collision-broadened line shapes contain a wealth of information about atmospheric properties: furthermore, collisions are the dominant broadening mechanism to much higher altitudes in the microwave region than at shorter wavelengths. Because of such advantages, passive microwave remote sens-

ing from satellites and ground stations has contributed uniquely and substantially to the study of atmospheric chemistry, meteorology, and global change.

The purpose of this volume is to present the state-of-the-art of passive microwave remote sensing to researchers and graduate students in other areas of remote sensing and atmospheric studies, as well as to those directly involved in this field. The overall scheme is to provide a collection of monographs that cover the most mature and representative applications of this approach to remote sensing, each prepared by a specialist who is at the forefront of ~~this~~ field. The primary emphasis throughout the volume is on fundamentals and method~~, which~~ will retain their values as new results from these applications supersede those presented here. Such results and the questions they address, of course, remain our ultimate motivation.

The applications are introduced by the first three chapters of the volume, which present the fundamentals of micro-wave radiative transfer, measurement techniques, and atmospheric propagation: Chapter 1 outlines the scope of the volume and introduces' the basics of radiative transfer and measurement techniques in the microwave region, with the objective of making the rest of the book intelligible to a reader with little or no background in microwave remote sensing. The specialized terminology of the microwave approach is introduced and quantitative relationships important to the subject are provided for general reference. The chapter also contains material of interest to the specialist; for example, it provides a careful treatment of the Rayleigh–Jeans approximation and its implications for remote sensing, this usually being neglected in the literature. The next two chapters build a foundation for understanding microwave propagation in atmospheres. Chapter 2 presents the current theory for microwave absorption by atmospheric gases, with emphasis on those constituents that have played roles in remote-sensing applications to the present, and Chapter 3 treats the more complex radiative transfer theory, ~~which~~ is requited to account for scattering in the presence of ~~rain~~.

The applications are literally presented from the ground up, beginning with remote sensing of the Earth's troposphere from ground stations and working outward to the solar family of atmospheres. The absorption spectrum of the Earth's troposphere is relatively simple and includes a few collision-broadened molecular absorption features in addition to nonresonant absorption by liquid water. The weakly absorbing water vapor line at 22 GHz, a strong oxygen band centered around 60 GHz, and more recently the strong 183-GHz water line are the most important features for tropospheric remote ensing These enable the determination of humidity and temperature structure using ground-based and satellite instruments, the techniques for which are discussed respectively in Chapters 4 and 6. The specialized case of the retrieval of variable radio-path delay through the atmosphere due to water vapor is an important subtopic in ground-based remote sensing, ~~which~~ is covered in Chapter 5.

By contrast, the Earth's upper atmosphere has a rich assortment of lines, particularly in the millimeter and submillimeter regions. Important molecules including ozone, water, carbon, and chlorine monoxide can be observed from the ground by viewing at wavelengths where the troposphere is partially transparent, Chapter 7 describes the techniques of microwave spectroscopy that arc used to study these

high-altitude constituents. Microwave spectroscopy is an extremely powerful tool for synoptic observation when given the vantage of an orbiting platform–the intervening troposphere is eliminated, which permits unimpeded observation of spectral lines at all frequencies, and the limb-sounding geometry ~~which~~ gives a great increase in both vertical resolution and sensitivity. This application is described in Chapter 8, which gives early results for the extremely important ozone and chlorine monoxide distributions measured by the Microwave Limb Sounder on the Upper Atmosphere Research Satellite, and explores the possibilities for more advanced instruments in the future.

The application of microwave remote-sensing techniques to the atmospheres of planets other than the Earth is discussed in the final two chapters. These atmospheres are of interest in their own right, but they also provide an invaluable test of our Earth-centered models and concepts. This aspect of microwave remote sensing is usually presented in the context of astronomy or space exploration, but the inclusion here emphasizes the close' connection to Earth-based remote-sensing techniques. Microwave spectroscopy of the ubiquitous CO molecule allows the winds and temperature structure to be traced in the Martian atmosphere and the upper Venus atmosphere, for example, and is discussed in Chapter 9. The insensitivity to clouds and the tendency toward simpler and weaker absorption at lower frequencies makes it possible to sound deeply into thick planetary atmospheres; indeed, microwaves are the only means to penetrate both the clouds and clear atmospheres of six of the eight major atmospheres of the solar system (Venus, Jupiter, Saturn, Uranus, Neptune and, arguably, Titan, as opposed to the Earth and Mars, where the atmosphere is transparent at many shorter wavelengths). As described in Chapter 10, the pressure-broadened absorption features of the deep planetary atmospheres are useful for determining the temperature structure and the distribution of microwave-absorbing condensibles.

This volume is the combined result of the efforts of all the contributing authors. They must take the credit for any success that has been achieved, whereas faults, oversights, and omissions are solely the editor's responsibility. I would like to express my appreciation to the series editor Jin Au Kong for his encouragement in my taking on this task, and to David Staelin for his accurate assessment of what that task entailed as well as his invaluable advice. I would like to thank the authors again for their assistance in reviewing other chapters than their own, and to others for their varied assistance: B. L. Gary, S. J. Keihm, C. S. Ruf, P. N. Swanson, R. R. Weber, W. J. Wilson, in addition to those who reviewed chapters at the request of individual authors. A special debt of gratitude is expressed to Steven J. Walter for his extensive, careful, and very helpful reviews of several of the chapters.

MICHAEL A. JANSSEN

Pacific Palisades, California
November 1992

(B) The work described in this publication was partially carried out at the Jet Propulsion Laboratory, California Institute of Technology, under a contract with the National Aeronautics and Space Administration.

1

AN INTRODUCTION TO THE PASSIVE MICROWAVE REMOTE SENSING OF ATMOSPHERES

MICHAEL A. JANSSEN

Jet Propulsion Laboratory
California Institute of Technology
Pasadena, California

1.1 A GENERAL PERSPECTIVE

This volume treats a specific topic in remote sensing. First, we consider only the microwave region of the spectrum and the use of microwave instrumentation. Second, we are concerned exclusively with the interpretation of passive measurements, leaving active approaches in this spectral regime such as probing by radar and occultation of spacecraft radio signals by an atmosphere to other volumes in this series. Finally. we take the study of atmospheres as the ultimate objective of our remote sensing. The restriction to passive measurements and atmospheres means that we deal almost exclusively with the interpretation of atmospheric thermal emission. As we will see, this gives a sharp focus to the radiative transfer problem and the central issue of this volume, the determination of atmospheric parameters from observational data.

The microwave region along with its major atmospheric emission sources is shown in the context of the electromagnetic spectrum in Figure 1.1. The microwave region generally spans the range from about 3 GHz (1 gigahertz = 10^9 Hz) to 300 GHz and above, although there is no wide acceptance of an exact range. or in particular, of an upper frequency limit. Terms that identify strictly spectral regimes are the centimeter. millimeter. and submillimeter regions. A useful criterion to identify the microwave region can be stated in terms of the technology

Atmospheric Remote Sensing by Microwave Radiometry. Edited by Michael A. Janssen
ISBN 0-471-628913

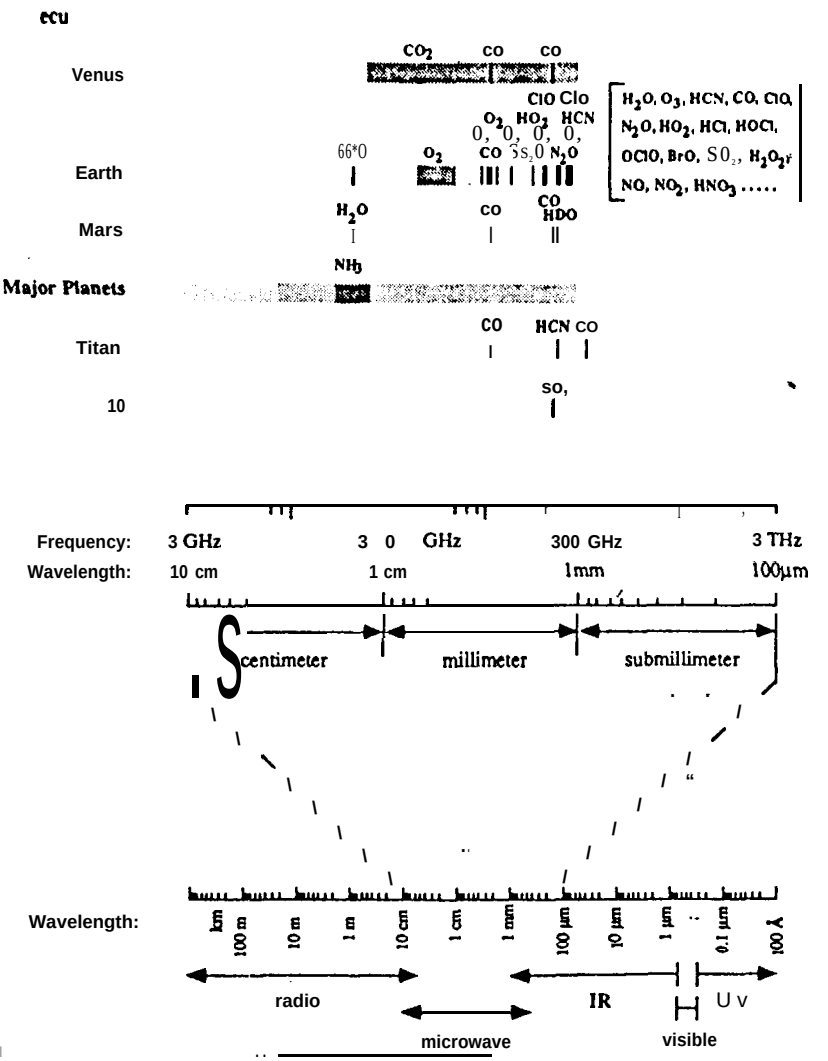

Figure 1.1. The microwave region spans at least two, and arguably three, decades between the radio and infrared regions of the electromagnetic spectrum. Gases responsible for absorption in the atmospheres of the Earth and the planets are indicated. The shaded band for Venus depicts nonresonant collision-induced absorption by CO_2, which increases with frequency. and extreme pressure broadening of the 24-GHz NH, inversion band leads to significant absorption at all microwave frequencies in the atmospheres of the major planets. All features identified in the centimeter and millimeter ranges have been used for remote sensing and are the focus for the applications presented *in* this volume. Remote sensing in the submillimeter region is in its infancy and some of the molecular absorption expected there are indicated.

and is consistent with its historical roots: it is the high-frequency extension of the radio range, with the upper end determined by the limits of the technology. The microwave approach is characterized in practical terms by the coherent detection of radiation, and this is generally the basis for the remote-sensing applications that are described in this volume.

Absorption of microwaves by atmospheric constituents provides the physical connection into an atmosphere that we exploit in various ways for remotely sensing its properties. Figure 1.1 shows the molecular absorption that have proven useful for remote sensing in the centimeter and millimeter regions-these absorption are described in detail in Chapters 2 and 8. The 22-GHz rotational line of water vapor and the spin-rotation band of oxygen centered around 60 GHz play dominant roles in the remote sensing of the Earth's troposphere, along with strong absorptiondue to liquid water when present in clouds or as rain. Nonresonant pressure-induced absorption by CO_2 accounts for most absorption in the deep atmosphere of Venus. and the inversion band of NH_3 centered around 24 GHz is the major absorber in the deep atmospheres of the outer planets. Coherent detection, as achieved by heterodyne receivers (see Section 1.3), allows atmospheric emission lines to be examined at the highest possible spectral resolution. Unique studies of the upper atmospheres of the Earth, Venus, and the tenuous atmosphere of Mars have been possible using high-resolution measurements of the millimeter lines of the indicated minor constituents.

We can look forward to heterodyne applications at frequencies possibly as high as 10 THz (1 terahertz = 10^{12} Hz) in coming years. Whether we stretch to include these as "microwave"' applications is not particularly important, although the remote-sensing applications developed for the millimeter region will apply directly to submillimeter lines, and in this sense we can consider the submillimeter region within the scope of this volume. Figure 1.1 indicates the variety of molecules that are accessible in this region, and the future possibilities for remote sensing of the Earth's upper atmosphere using their submillimeter lines are explored in detail in Chapter 8. The development of the submillimeter region will eventually open up new vistas in planetary studies as well.

The remote-sensing applications that take advantage of these absorption arc bound by both a common foundation in radiative transfer theory and a common technology. With the specialization to the microwave region, it is expected that most readers will be unfamiliar with the long-wavelength versions of these topics. namely. the microwave radiative transfer equation and techniques of microwave radiometry. These arc presented in the following two sections to provide a foundation for the rest of the volume.

1.2 THE MICROWAVE RADIATIVE TRANSFER EQUATION

The starting point for any passive remote-sensing application is the equation that describes the flow of radiant energy to be measured by a radiometer. The scalar form of this equation for atmospheric propagation is remarkably simple in the

Rayleigh–Jeans limit. and is sufficient to treat the large majority of microwave applications. We briefly outline the development of this equation on the assumption that the reader is familiar with basic concepts in radiative transfer, noting that more leisurely (and thorough) treatments can be found in several sources [1-5]. The emphasis in the following is to show where the standard approximations are made and what their implications are for our remote-sensing applications. A more general approach that includes scattering and polarization is outlined in Chapter 3 and also can be found in the sources referenced before.

1.2.1 Radiative Transfer in a Nonscattering Thermal Medium

The classical form of the radiative transfer theory was developed by Chandrasekhar [1]. The theory describes the intensity of radiation propagating in a general class of media that absorb, emit. and scatter the radiation. It is ideally suited for radiative transfer in media such as atmospheres in which the flow of energy plays the central role, and where such quantities as wave polarization or phase relationships play relatively minor roles or can be treated separately (for example. see Chapter 3 and Appendix 6A). The starting point of the theory is the description of the radiation field in terms of the specific intensity I_ν, which is the instantaneous radiant power that flows at each point in the medium, pcr unit area. per unit-frequency interval at a specified frequency, and in a given direction per unit solid angle. As illustrated in Figure 1.2, its variation at a point s along a line in the direction of propagation is obtained by considering the sources and sinks of the radiation in a volume element along that line. This leads to a differential form of the transfer equation,

$$\frac{dI_\nu}{ds} = -I_\nu\alpha + S \tag{1.1}$$

where α is an absorption coefficient, and S is a source term, which respectively describe the loss and gain of energy into the given direction.

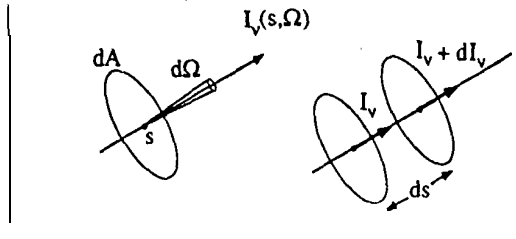

$$\text{I}\ dP = I_\nu dA\, d\Omega\, d\nu\ dI_\nu = -I_\nu \alpha ds + S\ d\ s$$

Figure 1.2. The specific intensity is the radiant energy flowing at each point in the medium per unit area normal to the flux. per unit solid angle, in the frequency range ν to $\nu + d\nu$. The variation of intensity with position is governed by an equation of transfer that takes into account the sinks and sources of radiation.

In the general theory, scattering into and from other directions can lead to both losses and gains to the intensity along a given direction and can be taken into account in the terms S and α. We will neglect scattering for the following, but will return later to the question of errors that this might introduce. Without scattering (o consider, the source term S needs to express only the locally generated contribution to the radiation. and the absorption coefficient α becomes a scalar characteristic of the medium that describes a true loss of energy from the radiation field into the medium, In particular, if we assume local thermodynamic equilibrium so that each point can be characterized by a temperature T. then the strict requirement of balance between the energy absorbed and emitted by any particular volume element leads to Kirchoff's law for the source term,

$$S = \alpha B_\nu(T) \tag{1.2}$$

where $B_\nu(T)$ is the Planck function:

$$B_\nu(T) = \frac{2h\nu^3}{c^2} \frac{1}{e^{h\nu/kT} - 1} \tag{1.3}$$

h is Planck's constant, k is Boltzmann's constant, c is the speed of light, and v is the frequency. The factor of 2 in the numerator accounts for both polarizations according to the usual convention. We note that By is sometimes considered as a surface brightness, which is the flow of energy across a unit area, per unit frequency, from a source viewed through free space in an element of solid angle $d\Omega$. Brightness and intensity have the same units, and Figure 1.3 demonstrates that the two are equivalent in this case. This argument can be extended to show that the intensity is generally invariant along any direction in free space, or in any region in which there are no local sources or sinks of radiation [3].

With the assumptions leading to Eq. 1.2 and the corresponding neglect of scattering in the absorption coefficient α, all terms of Eq, 1.1 depend only on the intensity along the path of propagation. Hence, the equation of transfer becomes a standard differential equation for which the complete solution is readily obtained. Substituting for S, we can write this solution as

$$I_\nu(0) = I_\nu(s_0)\, e^{-\tau(s_0)} + \int_0^m B_\nu(T) e^{-\tau(s)} \alpha\, ds \tag{1.4}$$

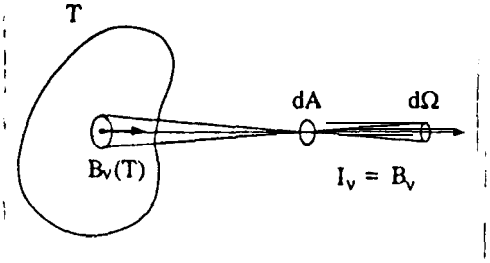

Figure 1.3. The surface brightness $B_\nu(T)$ of a blackbody emitter as viewed through free space in the solid-angle element $d\Omega$ produces a tfow of energy given by the specific intensity $I_\nu = B_\nu(T)$.

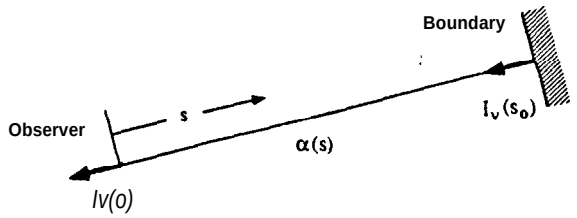

Figure 1.4. Assumed measurement geometry for the remote sensing of atmospheres.

where τ is the optical depth and is defined as

$$\tau(s) = \int_0^s \alpha(s')\, ds' \tag{1.5}$$

Anticipating the remote-sensing applications to follow, we have used the convention that the intensity is to be determined at the origin s = 0, where an instrument that measures the intensity is presumed to be located (see Figure 1.4). The integration then extends through the medium along the path of propagation and ends at some boundary s = so, where the condition is that the intensity has a starting value given by I_ν(s.).

1.2.2 Specializing to the Microwave Case

We introduce the microwave case by considering the low-frequency limit $h\nu \ll kT$. This is known as the *Rayleigh-Jeans limit* and allows the Planck function to be approximated as

$$B_\nu(T) \approx \frac{2\nu^2 kT}{c^2} = \frac{2kT}{\lambda^2} \tag{1.6}$$

where λ is the wavelength. The significant feature of this limit is the linear relationship of the Planck function with physical temperature. This naturally suggests a scaling of the intensity as

$$T_b(\nu) \equiv \frac{\lambda^2}{2k} I_\nu \tag{1,7}$$

We will use this expression to define* the microwave *brightness temperature* T_b, a quantity that will play the role of intensity in the radiative transfer equation but

● This is the Rayleigh-Jeans equivalent brightness temperature. and must be distinguished from the frequently-used thermodynamic definition—see Section 1 .2.4 for further discussion. Also, this definition sometimes appears without the factor of 2 in the denominator, in which case. the intensity I_ν refers to a single polarization of the radiation.

that has been dimensionally scaled to give units of degrees Kelvin. We emphasize that this definition is not an approximation in itself. and the implications of the departure of the Raylcigh-Jeans approximation from the Planck law arc developed later.

By using this definition. Eq. 1.4 can be rewritten as

$$T_b(\nu) = T_{b0}(\nu)e^{-\tau(s_0)} + \int^{s_0} \frac{T(s)}{\Re(\nu, T(s))} e^{-\tau(s)}\alpha\, ds \tag{1.8}$$

where the background brightness temperature T_{b0} is derived from our general boundary condition as

$$T_{b0} = \frac{\lambda^2}{2k} IV(s_0) \tag{1.9}$$

The factor

$$\Re(\nu, T) \equiv \frac{2kT}{\lambda^2}\frac{1}{B_\nu(T)} = \frac{kT}{h\nu}(e^{h\nu/kT} - 1) \tag{1.10}$$

and by using Eq. 1.7 in Eq. 1.3 can be seen to be just the ratio of the physical temperature T of a blackbody emitter to its brightness temperature T_b, namely,

$$\Re(\nu, T) = \frac{T}{T_b} \tag{1.11}$$

Expanding $\Re(\nu,T)$ in terms of $h\nu/kT$, we have

$$\Re(\nu, T) = 1 + \frac{1}{2!}\left[\frac{h\nu}{kT}\right] + \frac{1}{3!}\left[\frac{h\nu}{kT}\right]^2 + \cdots \tag{1.12}$$

where we see that $\Re$ is always greater than unity, and approaches unity in the Rayleigh-Jeans limit.

Equation 1.8 is exact as far as the Planck law is concerned. The Rayleigh–Jeans approximation is incorporated by setting $\Re = 1$, giving

$$T_b(\nu) = T_{b0}e^{-\tau(s_0)} + \int_0^{s_0} T(s)\, e^{-\tau(s)}\alpha\, ds \tag{1.13}$$

This is the form of the radiative transfer equation commonly used in microwave remote sensing. It is more accurate than one would expect at first glance; if one assiduously holds to the Rayleigh–Jeans approximation to include the calibration of a radiometer against blackbody targets, then this equation is actually correct to the first order in $h\nu/kT$ in spite of having neglecting this and all higher orders

when wc chose $\Re = 1$. The implications of the Raylcigh–Jeans approximation in this case and others are discussed further in Section 1.2.4.

1.2.3 Microwave Remote Sensing

The radiative transfer equation expressed in Eq. 1.13 is a simple weighted average over the physical temperature of an atmosphere. The emission $\alpha T\, ds$ from each element is attenuated by the factor e-' by the intervening medium as it travels toward the point of measurement. The sum of these contributions represents an average of temperature along the propagation path weighted at each point by $\alpha e^{-\tau}$. The radiative transfer equation expresses the forward problem: if the absorption and temperature are known along the path of propagation. then the brightness temperature can be computed from this equation.

In remote-sensing applications, we are ultimately concerned with the inverse problem. In particular. we start with measurements of the brightness temperature with the objective of Inferring the atmospheric properties that enter into the integrand of the radiative transfer equation. To illustrate the basic idea. let us consider two simple cases involving an atmosphere that we take to be isothermal at temperature T. From Eq. 1.13, we have

$$T_b = T \int_0^{\tau_a} e\text{-}r\ d\tau = T(1 - \text{e-}'") \tag{1.14}$$

where τ_a is the total optical depth through the atmosphere, and we have neglected the background term. If the optical depth is large, then we have for the first case

$$T_b = T\ (\tau_a \gg 1,\ \text{isothermal medium}) \tag{1.15}$$

In this case. we can think of a radiometer as a remote thermometer because its output is proportional to the temperature of the atmosphere. If the optical depth is small, on the other hand. we can approximate the result to give the second case:

$$T_b = T\tau_a \qquad (\tau_a << 1,\ \text{isothermal medium}) \tag{1.1.6}$$

If T *is* known. then in this case the optical depth τ_a is determined. Hence. the concentration of a particular constituent of the atmosphere can be obtained if it is the source of opacity and its absorption coefficient is known.

In the general case, the temperature structure, the opacity, or both are unknown. and the inverse problem becomes more difficult. If we think of T_b in a mathematical sense as a continuous function of the frequency, then we wish to solve the radiative transfer equation for an unknown function such as the temperature structure, $T(s)$, which appears in the integrand, and the inverse problem is seen to be that of an integral inversion. For example. if $T_b(\nu)$ and the opacity are known. then Eq. 1.13 is a linear integral equation–a Fredholm equation of the first kind—

that in principle can be inverted to obtain the temperature structure [6]. Realistically, the measurements of $T_b(\nu)$ are made in finite intervals of bandwidth centered on discrete points ν_i. If the desired result is also allowed to be discrete (e.g., temperatures at intervals of altitude), then the problem can be rephrased as a matrix inversion. In either case, the uncertainties encountered in the inverse problem are much harder to trace, As is well known in remote sensing, deeply based indeterminancies are present in the inversion-of integrals such as that in Eq. 1.13 or its matrix equivalent, and these can dominate even when measurement noise is vanishingly small, An excellent basic discussion of this point can be found, for example, in Twomey [7].

A more thorough discussion of the inverse problem in terms of the matrix formulation for the microwave case is given in Chapter 4, The practical approach to the inversion of Eq. 1.13 is usually unique to each application, however, and is a focus for the applications discussed in later chapters.

1.2.4 The Significance of the Approximations

The simple form of the radiative transfer equation given by Eq. 1.13 can be used for most applications without concern for the errors introduced by either the Rayleigh–Jeans approximation or the neglect of scattering. It is important to have a practical sense of where these errors arise and what they amount to, however, because these approximations are by no means universally valid in the microwave region. For example, deviations from the Rayleigh–Jeans approximation become more important as microwave remote sensing is extended to higher frequencies, and as applications at all frequencies become more exacting. Also, whereas typical cloud particles are not significant microwave scatterers, rain is, and is encountered frequently in tropospheric remote sensing.

The *Rayleigh–Jeans* Approximation

The definition of brightness temperature given by Eq. 1.7 is not unique. A quite different definition of brightness temperature is as the temperature of a blackbody radiator that produces the same intensity as the source being observed. The latter definition, which we will refer to as the *thermodynamic brightness temperature,* is given by the Institute of Electrical and Electronics Engineers [8], and is used in infrared work as well [9]. The first definition, which we will call the *Rayleigh–Jeans equivalent brightness temperature,* also appears in the literature [3, 10]. Unfortunately, many treatments avoid resolving this ambiguity by defining brightness temper-mum only after the Rayleigh-Jeans approximation has been introduced.

The relationship between the two definitions can be expressed for the emission from a blackbody radiator at temperature T as

$$\Re(\nu, T) = \frac{T_b \text{ (thermodynamic)}}{T_b \text{ (R-J equivalent)}} \qquad (1.17)$$

This difference can be significant not only at high frequencies, but also when the surface brightness of the source is very low, as in the case of the cosmic background radiation. The Rayleigh–Jeans equivalent brightness temperature is particularly appropriate in a radiative transfer context because it is simply a scaling of intensity, and radiative transfer integrals are sums over intensity. The thermodynamic definition can lead to confusion in this context. although it has the advantage that the connection to physical temperature is strictly maintained.

Figure 1.5 shows how $\Re$ depends on temperature and frequency. From this plot, we see that the fractional difference

$$\frac{T - T_b}{T_b} = \Re(\nu, T) - 1 \tag{1.18}$$

is small for either low frequencies or high temperatures. Of more concern in many applications, however, is the absolute difference

$$T - T_b = \frac{\Re(\nu, T) - 1}{\Re(\nu, T)} T \tag{1.19}$$

which is plotted in Figure 6. This difference actually increases with temperature, and approaches the limit $(T - T_b) \to h\nu/2k \approx 0.024\nu$ GHz. This difference can be significant throughout a large part of the microwave region..

Figure 1.6 demonstrates that the high-temperature asymptote of this difference is effectively reached at typical atmospheric temperatures, which is the main rea-

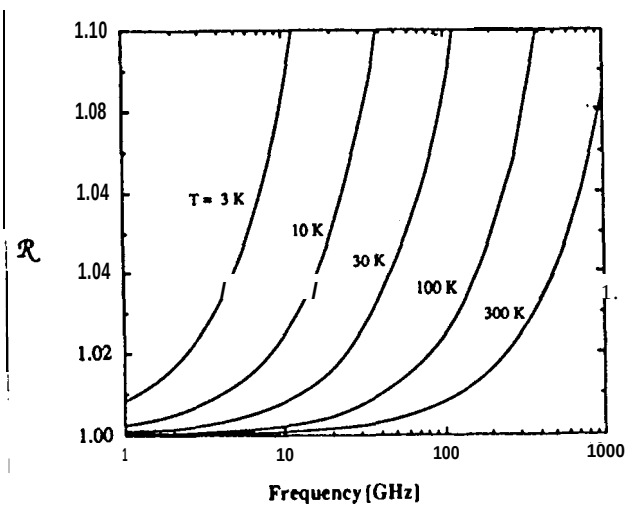

Figure 1.5. The ratio of thermodynamic brightness temperature (or physical temperature) to the Rayleigh-Jeans equivalent brightness temperature of a blackbody source due to deviation of the Rayleigh-Jeans approximation from the Planck law.

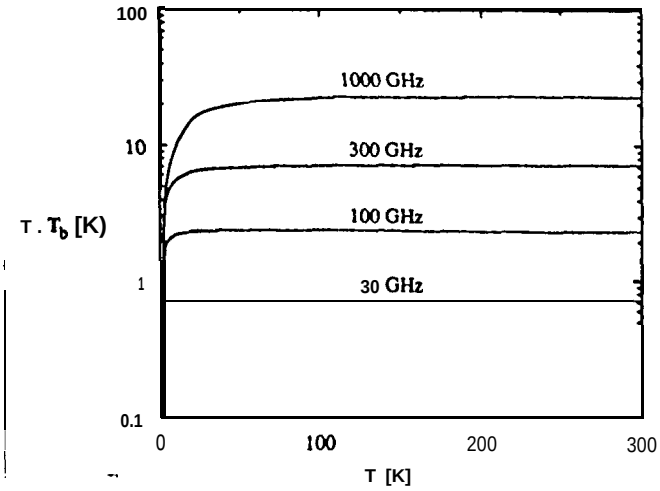

Figure 1.6. The absolute difference between physical temperature and the Rayleigh-Jeans equivalent brightness temperature Of a blackbody source.

son that corrections to account for the Rayleigh–Jeans approximation are so often ignored in microwave remote sensing. To illustrate, if we add a step between the more general radiative transfer equation expressed by Eq. 1.8 and its approximation in Eq. 1.13 by expanding the former to the first order in $h\nu/kT$, then we arrive at the expression

$$T_b(\nu) + \frac{h\nu}{2k} = T_0 e^{-\tau(s_0)} + \int_0^{s_0} T(s) e^{-\tau(s)} \alpha \, ds \qquad (1.20)$$

where T_0 is the physical temperature of a hypothetical blackbody "at the boundary. Now, if we calibrate a radiometer against blackbody targets and ignore all departures from the Rayleigh–Jeans law, then we effectively redefine brightness temperature as $T_b(\nu) + h\nu/2k$, and thereby recover the simple form of Eq. 1.13. Hence, the naive application of Eq. 1.13 automatically accounts for the first-order correction, and a simple calculation shows that it can be used under normal circumstances to frequencies up to 300 GHz with errors less than -0.1 K.

We caution that these approximations are no longer valid when the cosmic microwave background is present either as a cold-temperature reference or as the background term T_{b0}. For example, in the latter case, we can carry out the expansion leading to Eq. 1.20 for all but the background term, which we maintain exactly, and arrive at

$$T_{bc} = \frac{h\nu}{2k} \frac{(e^{h\nu/kT_c} + 1)}{(e^{h\nu/kT_c} - 1)} \qquad (1.21)$$

as the appropriate quantity to usc for T_0 in Eq. 1.20 (or for T_{b0} in Eq. 1. 13). where $T_c = 2.736 \pm 0.017$ K is the cosmic background temperature [11]. T_{bc} is also the appropriate value to usc as the cold-sky-reference brightness temperature if the thermodynamic temperature of the hot target is taken to be its brightness temperature. Note that T_{bc} is always greater than T_c, which is counterintuitive unless one remembers that wc are only supplying the higher-order adjustments to the first-order correction already made in Eq. 1.20, and made implicitly in the naive application of Eq. 1.13.

The Neglect of Scattering

The question of scattering is more difficult (o deal with in a quantitative way. This topic is thoroughly discussed in Chapter 3, and here we merely attempt to indicate a plausible limit inside of which scattering might be safely neglected. Let us take as a general criterion that the total power lost from the path of propagation due to scattering must be small compared to that involved in absorption or emission, keeping in mind that the notion of "small" ultimately depends on the experimenter and the case at hand. Specifically, let us consider scattering unimportant if the power lost from the beam due to scattering in each volume element is small compared to the power absorbed in that element, or, more conservatively, if the ratio of the scattering to absorption cross-section Q_s/Q_a is small for the scattering particles involved. If we consider that the reemitted power will be comparable to that absorbed, then the net fraction of the total radiance due to scattering that is ultimately measured will then be less than or equal to this ratio. This is particularly true if there arc other sources of absorption involved, and the condition can be overly conservative in some cases.

This condition is meaningful when considering liquid water, a strong microwave absorber that tends to dominate the radiative transfer process when it is present in even modest amounts in the form of clouds or rain. In Figure 1.7. we show the ratio Q_s/Q_a for single spherical water droplets of radius r that have been calculated using the frequency-dependent dielectric constant of water at a nominal temperature of 10"C [4]. The solid portions of the curves indicate the region where the Rayleigh scattering criterion $2\pi r << \lambda$ *is* valid, and the dashed upper region indicates the transition to the Mie scattering regime. The details of the Mie regime are not explicitly shown, but we note that the curves tend toward a value of order unity for $2irr >> \lambda$.

The upper limit for cloud droplet radii in the Earth's atmosphere is around 0.1 mm [12]. Thus, at the frequencies commonly used for remote sensing of the troposphere-about 20 to 90 GHz—absorption in liquid water cloud regions exceeds scattering by at least two orders of magnitude, and we would expect errors to be comfortably less than 1 % if we neglect scattering in the retrieval of temperatures in this frequency regime. The case becomes less clear for frequencies above 100 GHz, and scattering from cloud particles no longer can be ignored beyond 300 GHz. When cloud droplets coalesce to form rain, on the other hand, the resulting particle sizes approach the wavelength at all microwave frequencies. Drop-size distributions arc highly variable, with the mean drop radius tending to increase

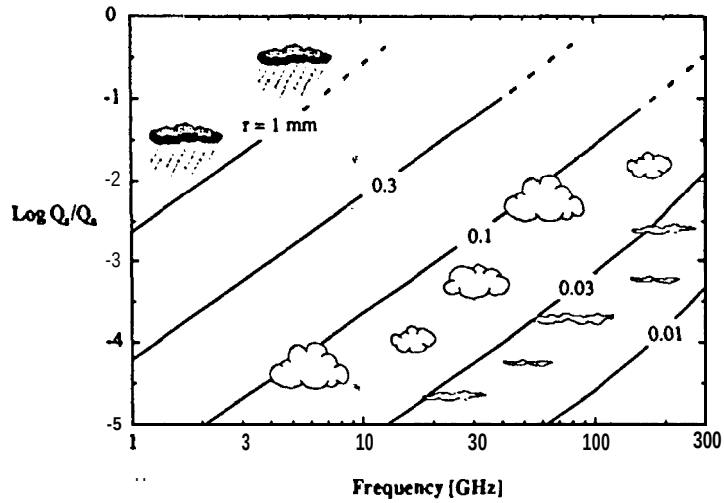

Figure 1.7. Ratio of scattering to absorption cross-section for water spheres of radius r. Typical droplet-size ranges are indicated for clouds with and without rain.

with rain rate-from 0.5 to 1.5 mm for light to heavy rainfall [12]. As indicated in Figure 1.7, these dimensions put the scattering problem well into the Mie regime at all microwave remote-sensing frequencies. Consequently, the applicability of the nonscattering radiative transfer equation becomes highly questionable when observing through regions containing rain, and results obtained under such conditions require the special considerations discussed in Chapters 3 and 6.

1.3 MICROWAVE RADIOMETRY

The objectives of this section are to describe how microwave radiometers work and to present the basic concepts involved in making radiometric measurements. A full presentation of the techniques of microwave radiometry is well beyond the scope of this volume, and the interested reader can pursue this subject in more depth in several texts [2,4, 13-15]. For our purposes, the function of a radiometer is to measure the radiant intensity (I_ν of the previous section), which, of course, is an idealized flow of power in infinitesimal elements of bandwidth and solid angle. In the following, we describe how the simplest radiometer-a total power radiometer-can be used to approximately measure the intensity over practical bandwidths and solid angles. This forms a basis for the topics of antennas, measurement uncertainty, and calibration. Finally, we describe the most common types of radiometers used in practice and discuss the current state of microwave technology.

Along the way. we introduce a working vocabulary so that the reader can follow discussions elsewhere that involve microwave radiometry. Italics identify the first use of each specialized microwave term, and a definition is given in context.

1.3.1 Fundamentals

A Simple ***Heterodyne*** *Receiver*

The typical microwave radiometer uses the so-called *heterodyne** principle, where both the technique and the terminology date from the early days of radio. A heterodyne receiver is one in which the received signal, called the *radio-frequency*, or *RF*, signal, is translated to a different and usually lower frequency (the *intermediate-frequency*, or *IF*, signal) before it is detected. The simplest version of a heterodyne radiometer is shown in Figure 1.8. It is an example of a *total power radiometer*. and illustrates features common to most microwave radiometers. Although this circuit is rarely used as it stands. it provides a useful introduction to both the theory and practice of microwave radiometry.

First, imagine that we have a signal at some frequency incident on the antenna of this radiometer. The purpose of the antenna is to couple this RF signal into a transmission line (a waveguide, for example), the function of which is to carry the RF signal to and from the various elements of the circuit. In the example. this signal is introduced directly into a *mixer,* which is a nonlinear circuit element in which the RF signal is combined with a constant-frequency signal generated by a *local oscillator.* or *LO [16].* Signals at various combination frequencies are produced at the output of this element because of its nonlinearity. These products include a signal whose frequency is the difference between the RF and LO frequencies, as shown schematically in Figure 1.9(a). This signal has the important property that its power is proportional to the power in the RF signal under the condition that the latter is much weaker than the LO signal. It is then filtered to exclude the unwanted products of the mixing, and amplified to produce the IF output signal.

Signals at microwave frequencies are often difficult or impossible to deal with directly, whereas a signal which has been *downconverted* to a sufficiently low IF frequency can be handled with a variety of techniques. After amplification and filtering. the power in the IF signal is measured with the use of a Second nonlinear element, a *square-law detector*. This element is typically a diode that operates

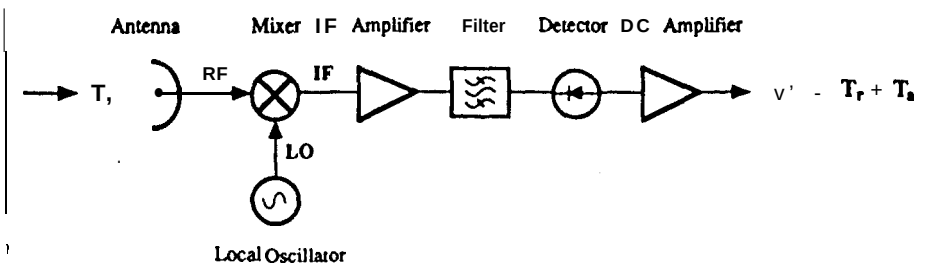

Figure 1.8. A schematic of the total power radiometer. This circuit produces an output voltage proportional to the received signal power. which is the principal function 01 a radiometer.

● Also called superheterodyne, where the original distinction is *now* obsolete.

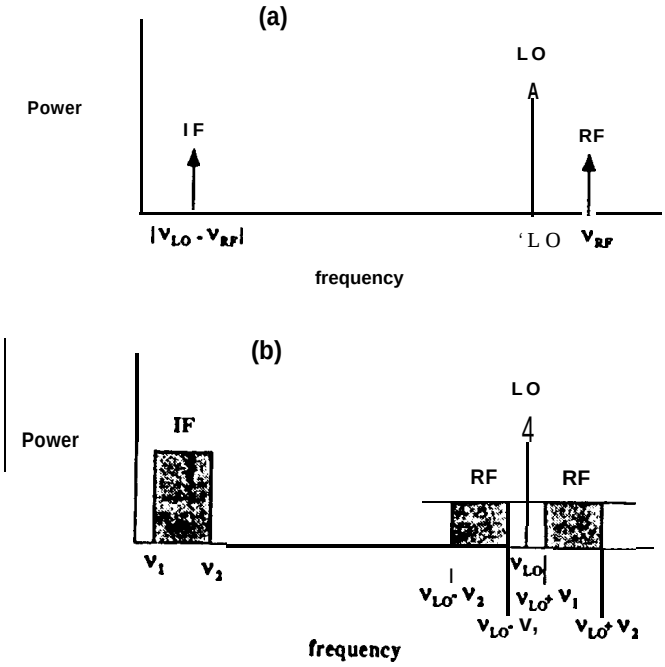

Figure 1.9. Frequency translation in heterodyne reception. (u) Monochromatic. signal (*b*) Broadband noise.

within its $i = \nu^2$ range and produces an output voltage that is proportional to the input power.

This example can be easily generalized to the case where broadband noise is received from a thermally emitting source. The mixer output then consists of a continuum of frequencies $|\nu_{LO} - \nu_{RF}|$ that corresponds to the frequencies ν_{RF} contained in the input noise signal, If the output is passed through a rectangular bandpass filter, the result will contain all frequencies originally present within two rectangular RF passbands that are images of the IF bandpass reflected around the LO frequency. This relationship is depicted in Figure 1.9(b), The two RF passbands are called the upper and lower *sidebands* of the receiver, which are effectively folded about the LO frequency by the mixer and translated into the IF band to create a *double sideband* receiver. As before, the detector then converts the net power in this band into a linearly related voltage.

A variation on this circuit that is becoming increasingly important is the use of direct RF amplification as this capability continues to develop at centimeter and long millimeter wavelengths. An amplifier immediately following the antenna, as shown in Figure 1.10, can be used to raise the power of the incoming signal well above the thermally generated noise power in the mixer or other following components. This can improve the radiometer sensitivity without requiring high performance in the mixer and the remainder of the receiver. Also, RF amplification

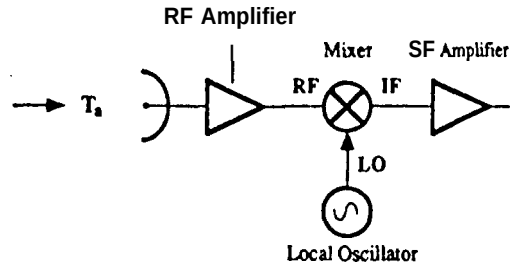

Figure 1.10. A receiver with direct RF amplification.

followed by a filter can be used to create a *single sideband* receiver if the RF power to appear in the desired sideband is amplified to a level well above that of its *image* band.

The Relationship of Received Power to Radiant Intensity

To account for the collection of thermal noise power by the antenna. we begin with Nyquist's law [17] for the noise power available from a *matched* resistor that terminates a transmission line (a matched element is one that reflects no power incident upon it). Nyquist's law is closely related to Planck's law, but is derived for the specific case of radiation propagating within a terminated transmission line instead of a general cavity [5, 18]. If the temperature of the matched resistor is T, then the power per unit bandwidth propagating from the resistor is*

$$P = kT \tag{1.22}$$

Let us now imagine that the transmission line is terminated by an antenna that is immersed in a uniform radiation field resulting from thermal blackbody emission at temperature T. For the moment, it is useful to think of an antenna as a matching device that couples the confined wave propagating inside the circuit to free space, and vice versa. The present case is then just a variation of Nyquist's hypothetical circuit, and the power per unit bandwidth that is coupled into the circuit must be equal to that propagating back to free space from the resistor. This power is thus also given by Eq. 1.22.

Now, as with radiant intensity and the definition of brightness temperature in the previous section, we use the approximately linear relationship between power and temperature to define the *antenna temperature:*

$$T_a \equiv P/k \tag{1.23}$$

as an appropriately scaled measure of the thermal power introduced into the receiver.

● In the Rayleigh-Jeans limit. For simplification. we carry this approximation through the remainder of this chapter, noting that the more exact case is easily recovered by dividing the right side of Eq. 1.22 by $\mathcal{R}(\nu, T)$.

The Antenna

The purpose of an antenna, beyond its function as an impedance-matching device between free space and the receiver, is to provide selectivity in the measurement of the angular distribution of the radiation. For an arbitrary distribution of radiant intensity with angle, $I_\nu(\theta, \phi)$, the net noise power entering the receiver is determined by the antenna and its sensitivity to direction. Some very general relationships exist between this angular distribution and the received power. As a shortcut to get at these, let us make the plausible assumption that the antenna is a linear device that couples the radiant power from a particular element of solid angle $d\Omega = \sin\theta\, d\theta\, d\phi$ into the receiver by the relationship

$$dP = A_e(f, \phi) I_\nu(\theta, \phi)\, d\Omega \tag{1.24}$$

where A_e is some linear coupling coefficient that depends only on the antenna and the direction of the incoming radiation. From the dimensions of this equation, A_e has units of area, and can be thought of as the effective area of the aperture for radiation incident from the direction of the solid angle element $d\Omega$. If the radiation field is caused by an extended source of incoherent radiation, such as thermal emission from an atmosphere, then the total power introduced into the receiver is the direct sum over all directions, or

$$P = \int_{4\pi} A_e(\theta, \phi) I_\nu(\theta, \phi)\, d\Omega \tag{1.25}$$

If we translate our units for power and intensity into temperature using the definitions for antenna temperature and brightness temperature given in Eqs. 1.23 and 1.7, then we obtain

$$T_a = \int_{4\pi} \frac{A_e(\theta, \phi)}{\lambda^2} T_b(\theta, \phi)\, d\Omega \tag{1.26}$$

We identify the quantity that multiplies T_b in the integrand as the *antenna gain*,*

$$g(\Omega) = \frac{A_e(\theta, \phi)}{\lambda^2} \tag{1.27}$$

This allows us to write a basic relationship between received power and the angular distribution of radiation as

$$T_a = \int_{4\pi} g(\theta, \phi) T_b(\theta, \phi)\, d\Omega \tag{1.28}$$

*The quantity that describes the antenna power pattern has several names and definitions that differ by a normalization constant, depending on the application. For example, the directivity of the antenna, or its directive gain, $G(\theta, \phi) = 4\pi g(\theta, \phi)$ is often used and gives the response of the antenna to radiation from a given direction relative to a hypothetical antenna with an isotropic power pattern.

We can interpret the antenna gain as the effective collecting area 01 the antenna. in units of wavelength squared. for radiation incident on it from the direction of the solid angle element $d\Omega$. Note that from the thermodynamic argument of the previous section, wc must have

$$\int_{4\pi} g(\theta, \phi)\ d\Omega = 1 \qquad (1.29)$$

To achieve selectivity in direction, a practical gain pattern will consist ofa well-defined main beam with much lower gain away from the beam axis. A useful quantity to describe the angular resolution of such a pattern is the *main-beam solid angle*, which we define as

$$\Omega_a = \int_{4\pi} \frac{g(\Omega)}{g(o,\ o)}\, d\Omega \qquad (1.30)$$

where the angular coordinate system is assumed to be centered on the peak gain, $g(0, 0)$. For example, if the gain has a constant value over some solid angle and is zero outside, then the foregoing just returns that solid angle. An important relationship is obtained by using Eqs. 1.29 and 1.27

$$\Omega_a = \frac{\lambda^2}{A_e(0, O)} \qquad (1.31)$$

The effective area in the direction of maximum gain, $A_e(0, O)$, is usually just called the *effective aperture* area, A_e. To the extent that area A_e can be related to the size of a physical aperture, Eq. 1.31 characterizes a diffraction-limited optical system. For example, if we associate a diameter D with the effective aperture A_e such that $A_e = \pi D^2/4$ and a beam diameter θ_a such that $\Omega_a = \pi\theta_a^2/4$, then Eq. 1.31 reduces to

$$\theta_a = \frac{4}{\pi}\frac{\lambda}{D} \qquad (1.32)$$

It is interesting that we can derive this relationship without recourse to wave-optics arguments or reference to a specific antenna geometry. The details of the gain pattern and its actual relationship to the physical aperture, of course. must be obtained using Maxwell's equations with the appropriate boundary conditions. A familiar point of reference for a diffraction-limited aperture is the diffraction pattern given by a uniformly illuminated circular aperture, for which the angular diameter of the first null of the interference pattern (the Rayleigh criterion) is approximately $1.22\lambda/D$. More generally, most microwave antennas can be approximated as a planar aperture with a spatially varying illumination, or field distribution. The angular distribution of outgoing power is then the Fourier transform of the autocorrelation of this aperture field distribution [2].

An important class of microwave antenna is the horn *antenna*, so-called because of its shape. In its simplest version, this need be little more than a section of waveguide with a uniformly expanding cross-section that is open at its wide end: The smooth taper of the walls minimizes reflection as an outgoing wave gradually expands to become a wave in free space. Horn exit apertures are rarely more than a few wavelengths in diameter, so their beamwidths typically exceed several degrees. The effective aperture illumination is not uniform, but is naturally tapered so that the field approaches zero at the horn rim. This has two consequences because of the Fourier relationship between aperture illumination and gain pattern: the main beam is broadened because the aperture illumination is effectively narrowed, and the interference fringes away from the main beam (or *sidelobes*) are reduced because of the lack of a sharp discontinuity in the illumination. With good design, it is possible to create an illumination across the horn exit aperture that is approximately Gaussian so that the sidelobes virtually disappear. More elaborate versions (*scalar horns*) are possible that ensure azimuthal symmetry of the resulting power pattern even though the input waveguide and its internal field distribution are not symmetric.

Horns can be used *as feedhorns* to illuminate large apertures, which give much higher angular resolution, Such antenna systems are often analogous to those familiar at optical and infrared wavelengths. For example, a parabolic reflector illuminated by a feedhorn is essentially a Newtonian telescope; Cassegrain and other multiple reflector systems are also common [2, 19-23]. These kinds of antennas provide resolutions from a few degrees down to a few arc minutes. Finally, aperture-synthesis techniques are possible in which large virtual apertures are created from assemblies of smaller real apertures [24]. This approach has made possible the study of distant radioastronomical sources at milliarcsecond resolution, and is important for the study of planetary atmospheres (see Section 1.3.3 and Chapters 9 and 10). Synthetic apertures have other implications for remote sensing [25, 26], and, for example, may eventually provide the large apertures needed for high-resolution Earth observations from geosynchronous orbit [27].

A somewhat arbitrary but standard measure of resolution for microwave antennas is the *half-power beamwidth* (*HPBW*), or the diameter of the gain pattern where its value is half that of the central peak (also used for the same purpose is the term Full Width at Half-Maximum, or *FWHM*). For example, the uniformly illuminated circular aperture of diameter D has a HPBW of $1.02\lambda/D$. The typical tapering of the aperture illumination on a microwave aperture of diameter D tends to increase the beamwidth and lower the sidelobes relative to this case. Microwave antennas used for remote sensing have half-power beamwidths in the range 1.3–$1.7\lambda/D$, depending on compromises made by the antenna designer. Hence an approximation that describes the beamwidths of most antennas to an accuracy of about 10% is

$$\theta_{\text{HPBW}} = 1.5\lambda/D \tag{1.33}$$

Figure 1.11 shows a plot of this rule-of-thumb beamwidth versus aperture size for microwave frequencies. Antennas built for communications systems are usually

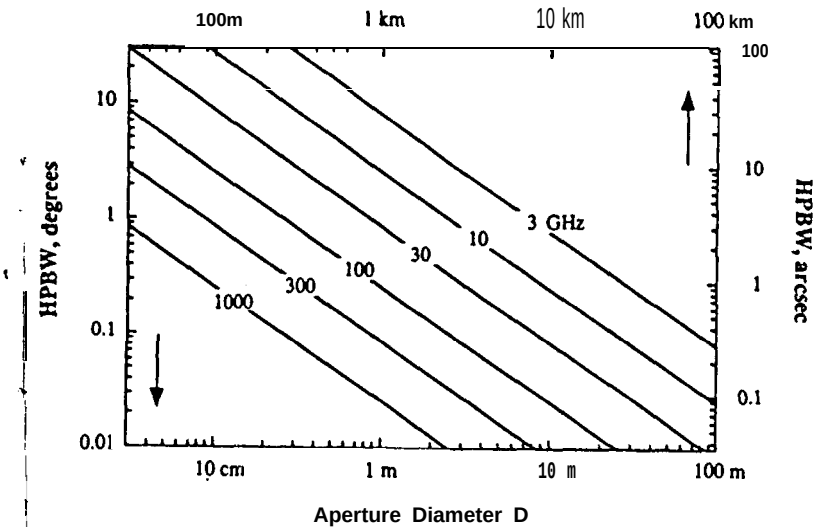

Figure 1.11. Relationship of aperture size D to half-power beamwidth as a function of frequency for a nominally illuminated antenna (from the approximate relationship in Eq. 1.33). The lower horizontal axis gives aperture sizes typical of filled-aperture antennas. These provide angular resolutions read on the left-hand vertical axis. The upper horizontal scale gives aperture sizes in the domain of aperture-synthesis techniques and yield resolutions read on the right-hand vertical axis.

optimized for peak gain and tend to have narrower main beams for a given aperture diameter than this relationship implies because the increased sidelobes are of less concern in this application [23].

Because of wavelength, physical sizes of microwave antennas need to be much larger to achieve the same resolution as apertures at infrared or optical wavelengths. Antenna size is an important practical concern in many microwave applications as a result.

Calibration

The receiver output voltage must be calibrated in units of antenna temperature. This involves finding both a gain coefficient and an offset, where an offset is needed to account for power generated within the receiver itself. Received power is inevitably lost by absorption as it passes through successive stages of the receiver—the elements that are responsible for this loss reradiate power at their own physical temperature, and if this occurs before or within the mixer and the first stages of the amplifier, this power will be amplified along with the signal (in many radiometers. this internally generated power exceeds that of the signal), The net IF power reaching the square-law detector then consists of two components: (I) that which represents the amplified signal power and is proportional to the antenna temperature T_a, and *(2)* the internally generated power, which we identify as the *receiver temperature* T_r with the understanding that it is to be calibrated on the same scale as the antenna temperature. The sum of these components is called the

system temperature,

$$T_s = T_a + T_r \tag{1.34}$$

As demonstrated *in* Figure 1.12, we can calibrate the radiometer and determine the offset at the same time by observing blackbody emitters at two different temperatures. For example, we can enclose the field of view of the antenna with a temperature-controlled microwave absorber (or *load*) at each of two temperatures, T_{hot} and T_{cold}. If the radiometer is linear, which is usually well approximated in practice, then we can determine the antenna temperature T_a for a target at an unknown temperature as

$$T_a = c(V - V_0) \tag{1.35}$$

where V_0 is the voltage offset due to the receiver temperature (e. g., $T_r = V_0/c$), and the radiometer calibration constant c is determined as

$$c = \frac{T_{hot} - T_{cold}}{V_{hot} - V_{cold}} \tag{1.36}$$

where the voltages V_{hot} and V_{cold} are the measured output voltages for the respective T_{hot} and T_{cold} loads.

The Radiometer Noise Formula

Any measurement of noise power possesses an inherent statistical uncertainty that depends on the bandwidth B of the noise power and on the time t allowed for its

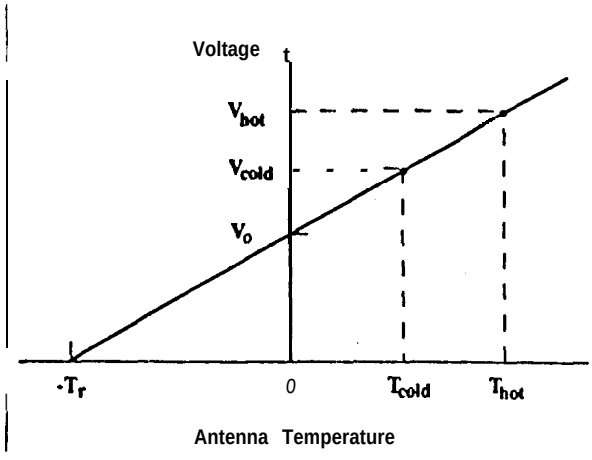

Figure 1.12. Calibration of antenna temperature using a hot and cold load. The calibration coefficient is given by the measured slope, and the voltage intercept for zero antenna temperature determines the receiver temperature T_r.

measurement. A simple way to visualize this dependence is to consider the noise power as a time-varying voltage that corresponds to bitnd-limited white noise (within a reasonably narrow bandpass, thermal noise contains approximately the some average power in every frequency interval: if the signal is passed through a rectangular bandpass filter. it will contain the same average power in every frequency interval within the bandpass and zero outside it). A typical measurement consists of the square-law detection of this signal followed by an averaging for time t. The Fourier representation of a band-limited white-noise signal over time interval t consists of $n = Bt$ components with coefficients whose absolute values are normally distributed with a uniform standard deviation. If we follow the detection and averaging process mathematically using the Fourier representation, then the measurement will be proportional to the sum of squares of the coefficients, and will be uncertain because of the uncertainty of the components that comprise it. The relative uncertainty AP/P in the sum P can be shown to be inversely proportional to the square root of the number of coefficients [13, 28], or

$$\frac{\Delta P}{P} = \frac{1}{\sqrt{n}} = \frac{1}{\sqrt{Bt}} \tag{1.37}$$

Now, P and A P are, respectively, proportional to the system temperature T_s and the uncertainty of the measurement AT, so that we readily obtain the noise formula

$$\text{'T} = \frac{T_s}{\sqrt{Bt}} \text{(total power radiometer)} \tag{1.38}$$

Figure 1.13 shows how the uncertainty of a 1-second measurement depends on system temperature and bandwidth for both this case and the Dicke-switched radiometer discussed in the next section.

1.3.2 Two Common Types of Radiometers

The Dicke Radiometer

The total power radiometer is not well suited for many applications because it is difficult to stabilize and calibrate. To appreciate the importance of gain fluctuations, consider as a typical case a total power radiometer with a system temperature of 500 K and a bandwidth of 100 kHz. According to the noise formula, the uncertainty of a l-second measurement made with this radiometer would be 0.05 K. or one part in 10^4 of the total noise power. Because the gain acts on the total power, the stability of the radiometer would have to be held to one part in 10^4 so that gain fluctuations do not dominate the sensitivity of the instrument. Such stability is difficult to achieve. A general solution to this problem is the *Dicke radiometer* shown schematically in Figure 1.14. A switch follows the antenna in this circuit, which allows the receiver input to alternate between the antenna and a stable source of therrmd-noise power provided by a reference load. A reference load can be an

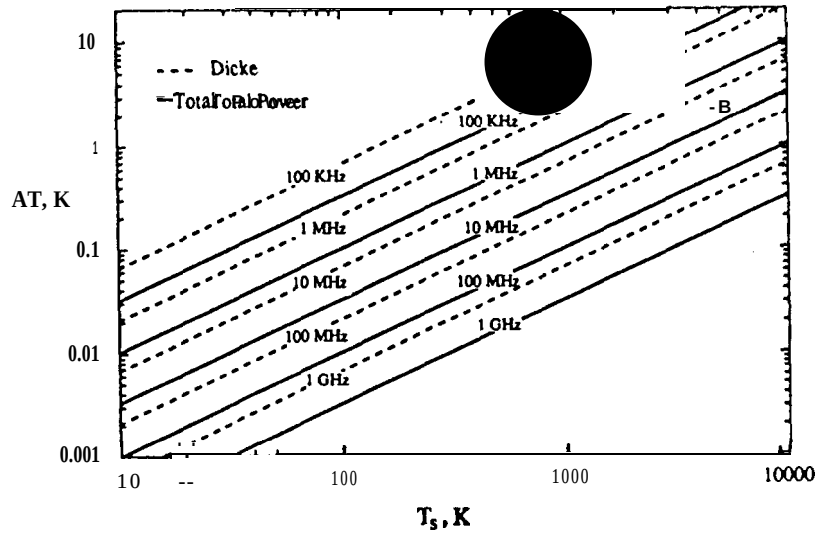

Figure 1.13. Uncertainty (standard deviation) of a 1-second measurement as a function of system temperature and bandwidth. The values shown are from Eq. 1.38 for a total power radiometer and Eq. 1.39 for a Dicke-switched radiometer.

external load viewed by a second antenna or a load internal to the circuit. with the load maintained at a known temperature in either case. As the switch alternates position, the output voltage of the Dicke radiometer correspondingly alternates between the total powers from the antenna and the reference load. The receiver is followed by a *synchronous detector*, or *lock-in amplifier*, which rectifies the switched signal so that the output is proportional to the difference between antenna

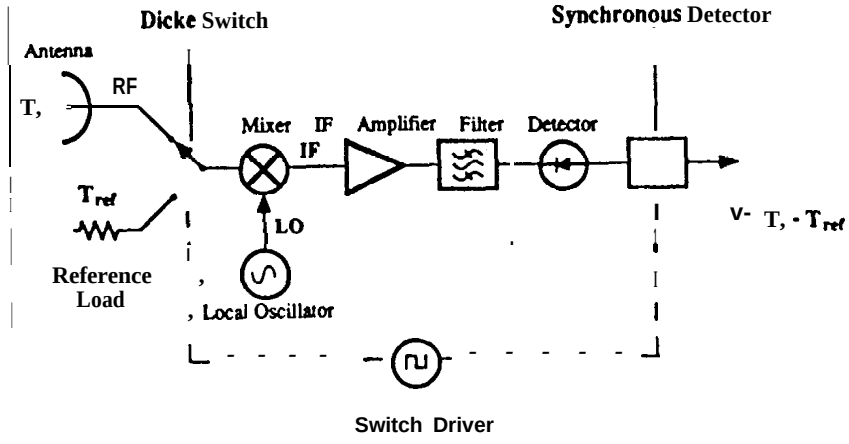

Figure 1.14. Schematic of a Dicke radiometer.

and load temperatures. If the switching time is much shorter than the characteristic period of the gain fluctuations. then the gain fluctuations cause only the measured temperature difference to vary. Their effect is, therefore. reduced by the ratio of the measured temperature difference to the total power, which can bc made quite small in many cases.

The measurement uncertainty for a Dicke radiometer that divides its time evenly between ihc source and a reference of comparable temperature is

$$\Delta T = \frac{2T_z}{\sqrt{Bt}} \quad \text{(Dicke radiometer)} \tag{1.39}$$

The factor-of-2 increase relative to the uncertainty of the total power radiometer follows because the net integration time *on* the source is reduced by half, and because two equally uncertain quantities are difference to form the result, where each consideration increases the uncertainty by a factor of root 2. The formula is more complicated but easily derived if the source and reference temperatures are significantly different [4].

The stable components and amplifiers of modem solid-state electronics have reduced the need for rapidly switched Dicke radiometers, and have even made total power radiometers practical in some applications. Nevertheless all radiometers are designed to measure, in one way or another, the difference between the desired antenna temperature and that of a reference source. For example. total power radiometers with movable external targets or switched beams use the basic principle of a Dicke radiometer and can achieve the same stability under some circumstances. The term ' 'Dicke radiometer'" is usually reserved for radiometers with an internal switch, however.

The Microwave Spectrometer

Many applications depend on the measurement of the spectral dependence of the emission. A microwave *spectrometer*, or spectral line receiver, is obtained by subdividing the IF passband of any of the prior radiometers and separately detecting the output of each resulting segment. The hetérodyne technique allows the spectral region of interest to be placed at a convenient frequency for this analysis. The IF passband can be subdivided as indicated in Figure 1.15 by using a bank of narrowband filters with the desired distribution of bandpass characteristics; alternatively, digital sampling and autocorrelation or other techniques of spectral analysis can be used, There is no effective upper limit to the resolution and number of frequency elements that can be obtained. As an extreme case. for example. one spectrum analyzer recently built for signal processing contains 8.4 million contiguous channels with O. OS-Hz resolution [29]. However, there is a practical limitation when the spectral feature to be analyzed is so broad that it exceeds the practical IF bandwidth of a radiometer. An example is the 22-GHz water-vapor line in the Earth's troposphere. Such a feature must bc observed with the equivalent of a single-frequency radiometer that canbe tuned to a number of frequencies.

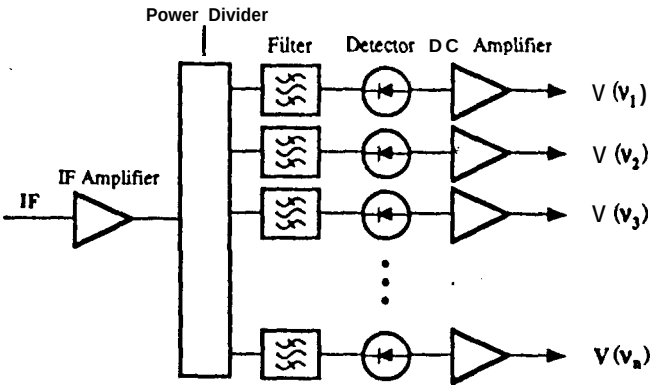

Figure 1.15. Schematic of a microwave spectrometer constructed with bandpass filters.

The accuracy of the frequency measurement also has no practical limit. Local oscillators at all microwave frequencies can be phase-locked to reference frequencies derived from time standards. Hence, it is possible to control the radiometer frequency to tolerances well below 1' Hz throughout the microwave range, which is far more accurate than needed for any remote-sensing application discussed in this volume. The ideality of microwave spectroscopy for both frequency accuracy and resolution makes this approach a very powerful tool for atmospheric remote sensing.

The simplest spectrometer system uses a double sideband receiverin which the spectral feature to be observed is folded into the IF passband with an image RF passband that contains no useful signal. In this case, the signal power is divided in ha] f in the IF band relative to the net noise power and a *single-sideband receiver temperature* is conventionally defined to be twice as large as the system temperature T, of Eq. 1.34. The single-sideband temperature is the appropriate quantity to use in the noise formula of Eqs. 1.38 or 1.39 to determine the measurement uncertainty.

1.3.3 About Hardware

It is impossible to capture the state of microwave technology in a few pages, and the rapid development of this field would quickly date the attempt. However, we can introduce the main concepts and define terms likely to be encountered in the literature. We begin with the main building blocks that are available to the circuit designer, and follow with some examples of radiometer design.

Circuit Elements

Waveguide. The power radiated by an oscillating current increases as the square of the frequency. so that the usual view of a circuit as currents flowing in conduc-

tors becomes instead. at high frequencies, a radiation field controlled by appropriate boundary conditions. As a result, conventional circuits with wires are not feasible in the microwave region except when physical sizes are kept very small. Waveguide is commonly used as the basic signal-carrying medium at frequencies up to about 100 GHz. beyond which it becomes impractical for general usc because of increasing attenuation and increasingly severe mechanical tolerances. Waveguides for passive systems are made in standard sizes for frequencies up to about 100 GHz. which are rectangular with a width-to-height ratio of 2:1. This geometry permits them to carry a single mode (TE_{10}) over a wide frequency range: multiple-mode transmission is undesirable because the performance of most circuit elements is rapidly degraded by mode mixing. The set of standard sizes gives overlapping single-mode transmission capability up to about 100 GHz. Table 1.1 lists the waveguide *bands* that are coordinated with these standard sizes. The band nomenclature is intentionally obscure because it is derived from code designations originating from classified radar development during World War II.

Passive Components. Many circuit elements can be constructed using waveguide geometries [30, 31]. *Power dividers* split the incoming power evenly into exit ports: the outputs can be in phase or out of phase according to the design. *Directional couplers* can transfer a desired amount of signal propagating in a given direction in one waveguide to another. A smoothly tapered resistive vane inserted into a waveguide parallel to the TE_{10} mode E-field can provide a nonreflecting *attenuator*, and a resisting material similarly tapered to eliminate reflections and placed to absorb all the entering power provides a *matched load.*

The novel properties of ferrites lead to a valuable class of microwave components. Ferrites comprise a class of nonconducting ceramiclike materials with the general composition $MO \cdot Fe_2O_3$, where M represents a divalent metal such as magnesium or iron. When a strong magnetic field is used to align the unpaired

TABLE 1.1 Standard Microwave Band Nomenclature

Band Designation	Nominal Frequency Range (GHz)
L	1-2
S	2-4
C	4-8
X	8-12
K_u	12-18
K	18-27
K_a	27-40
Q	36-46
V	46-56
W	56-100

electrons in a ferrite. a wave propagating in this material experiences Faraday rotation: tor example. the polarization of a linearly polarized wave traveling parallel to the magnetic field vector rotates in a sense determined by the direction of the magnetic field. The ferrite medium is nonreciprocal because the absolute sense of this rotation is the same for waves propagating either parallel or antiparallel to the magnetic field. This property has been exploited in waveguide geometries to produce nonreciprocal microwave components such as *isolators*, two-port devices in which a signal passes unimpeded in the forward direction, whereas a wave traveling in the reverse direction is rotated into an attenuator and absorbed. Isolators are used to ensure good matches in circuits that are especially sensitive to reflections. A three-port *circulator is* a device that passes a signal input to port I to port 2, port 2 to 3, and 3 to 1; circulators can be made with more than three pens. A *ferrite switch* can be made by controlling the direction of circulation in a three-port circulator with an externally applied magnetic field. A *latching* ferrite switch can be made by reversing the intrinsic magnetization of the ferrite with a pulsed current in an external coil; such switches routinely achieve microsecond switching times and are particularly valuable as the switching elements in Dicke radiometers.

Mixers. Waveguide techniques can be used to couple microwaves into and out of solid-state elements to produce a variety of active circuit components. Mixers are typically three-port devices that concentrate the microwave signal and local oscillator power entering through two ports as currents across a diode, while the IF power is drawn out through a third port. Considerations in the construction of a mixer include the matching of all three ports and the efficient conversion of the signal power to IF in the face of parasitic impedances that become prevalent at high frequencies. Smallness is a virtue in minimizing such impedances. and small area junctions such as arc possible with Schottky-barrier diodes are important. The latter possess nearly ideal i-v curves and are extensively used in microwave applications. Other nonlinear elements such as Josephson junctions are finding increasing use at high frequencies.

Sources. The earlier generation of oscillators was based on properties of electron beams, 'which could be controlled to make devices such as klystrons and traveling-wave tubes. Such devices were intrinsically bulky, often short-lived. and required extensive supporting equipment such as high-current and high-voltage supplies. The discovery in 1963 of the oscillatory properties of bulk n-type GaAs and InP materials when subjected to a static voltage led to the *Gunn oscillator [32],* a solid-state device that has now almost universally replaced electron-beam devices as local oscillator sources in radiometers. Gunn oscillators have greatly simplified the practice of microwave radiometry. They can be phase-locked to standard frequencies and are readily available at frequencies up to 100 GHz, which appears to be a practical upper limit. LO signals are provided at higher frequencies by *frequency multipliers.* or devices that use the nonlinear properties of waveguide-mounted diodes to produce selectively enhanced harmonics from lower-frequency oscillators.

Wuvcguidc-mounted avalanche diodes can be used to produce broad-band white noise with equivalent blackbody temperatures well in excess of their ambient temperatures (e.g., by factors of 100 or more). Such *noise diodes* provide a useful calibration signal when injected weakly into a radiometer through a directional coupler. The stability of such calibration signals can be much better than 1 % when the diode voltages and physical temperatures arc well-controlled.

RF Amplifiers. A number of approaches have been developed in recent years for direct amplification at microwave frequencies. Cryogenic amplifiers such as masers or cooled ***HEMTs*** *(high-electron-mobility transistors)* can produce significant gain with excellent efficiency so that very low system temperatures can be achieved. Maser amplifiers using pumped ruby have set the standard for low-noise communications in the centimeter wavelength range [33]. Development of solid-state amplifiers such as HEMTs has been relatively recent but rapid, and useful amplification has been achieved at frequencies as high as 100 GHz [34, 35].

Quasi-Optical Elements. Quasi-optical techniques arc often used in the short-millimeter and submillimeter ranges where waveguides become impractical [36, ,37]. Directed radiation in free space with a Gaussian intensity distribution perpendicular to the axis of propagation remains collimated over useful distances, and is easily formed by a scalar feed with a parabolic reflector. This *beam-waveguide* approach makes possible a variety of interesting circuit components such as frequency diplexers and filters. Gaussian beams are diffraction-limited and represent the long-wavelength limit of geometric optics; indeed, many quasi-optical devices such as Fabry-Perot diplexers are directly analogous to optical devices. Such techniques are fundamental to pioneering developments in terahertz receiver technology, which may someday extend the microwave approach to frequencies as high as 10 THz [37].

Radiometers

Microwave radiometers are as varied in their design as the applications for which they were developed. Considerations at a given frequency include performance factors such as sensitivity, accuracy, and spatial resolution (usually desired to be as high as possible), which must be balanced against opposing factors such as complexity, weight, size. and power (which ultimately determine the price to be paid). The receiver temperature T_r is a key performance factor in many applications, particularly in microwave spectroscopy and radio astronomy. Figure 1.16 shows single-sideband receiver temperatures that have been achieved to date as a function of frequency [38. 39]. The best performance at frequencies up to roughly 50 GHz is given by cryogenic systems using masers and cooled HEMTs for direct RF amplification, and by S1S (superconductor-insulator-superconductor) mixers farther into the millimeter and submillimeter regions. Such systems tend to be complex because of their cryogenic needs. Uncooled Schottky diode mixers are

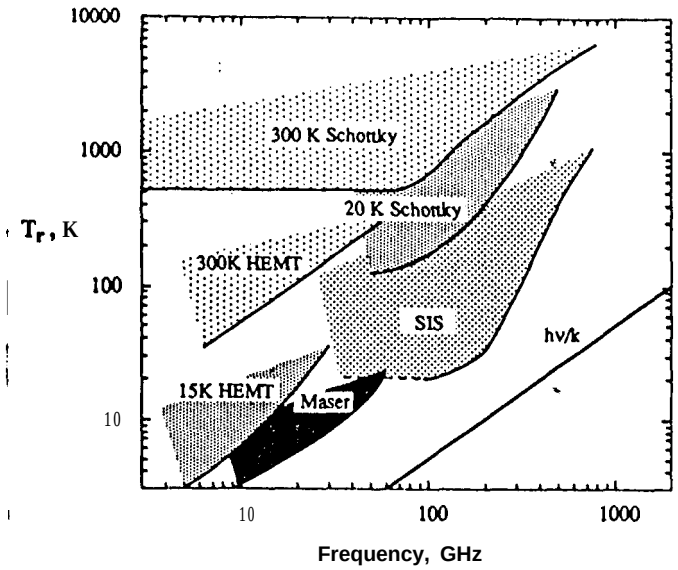

Figure 1.16. Single-sideband~~empemwrcscurrently achieved in the microwave region. Heterodyne receivers using Schottky-barrier diode mixers can be used at ambient temperature or cryogenically cooled [35,38]; cryogenic S1S (superconductor-insulator-supmconductor) Josephson junctions can be used as the mixing elements in heterodyne receivers 10 achieve very low system temperatures [39]. Direct-amplification receivers can be built using masers [33] and cooled or uncooled HEMT (high-electron-mobility transistor) amplifiers [35]. The quantum noise limit is $h\nu/k$.

/receiver

adequate for most broadband applications at frequencies well into the millimeter region, because the signal is of the same approximate magnitude as the typical receiver temperature (for double-sideband applications, the receiver temperatures shown in Figure 1.16 should be divided in half). Uncooled HEMT amplifiers exhibit excellent performance to 100 GHz, and their full potential for radiometry is just beginning to be exploited.

Examples of the current generation of radiometers built for atmospheric remote sensing are shown in Figures 1.17 and 1.18. The first is a ground-based water-vapor radiometer built to measure the tropospheric water vapor and cloud liquid burden from atmospheric emission in the vicinity of the 22-GHz H_2O line [40; see also Chapter 4]. This system was built to be portable and inexpensive while provialing state-of-the-art accuracy in radiometry, and has been used in support of atmospheric radio-path-delay correction for geodesy (see Chapter 5). Figure 1.18 shows the most recent of the many radiometers that have been placed into Earth orbit to sense atmospheric temperature and water on global scales (see Chapter 6 and Table 6.1).

The study of the atmospheres of other planets requires a radioastronomical approach because the apparent disks of planets with major atmospheres range in diameter from about one arc-minute (Venus) to less than 3 arc-seconds (Neptune).

Short.

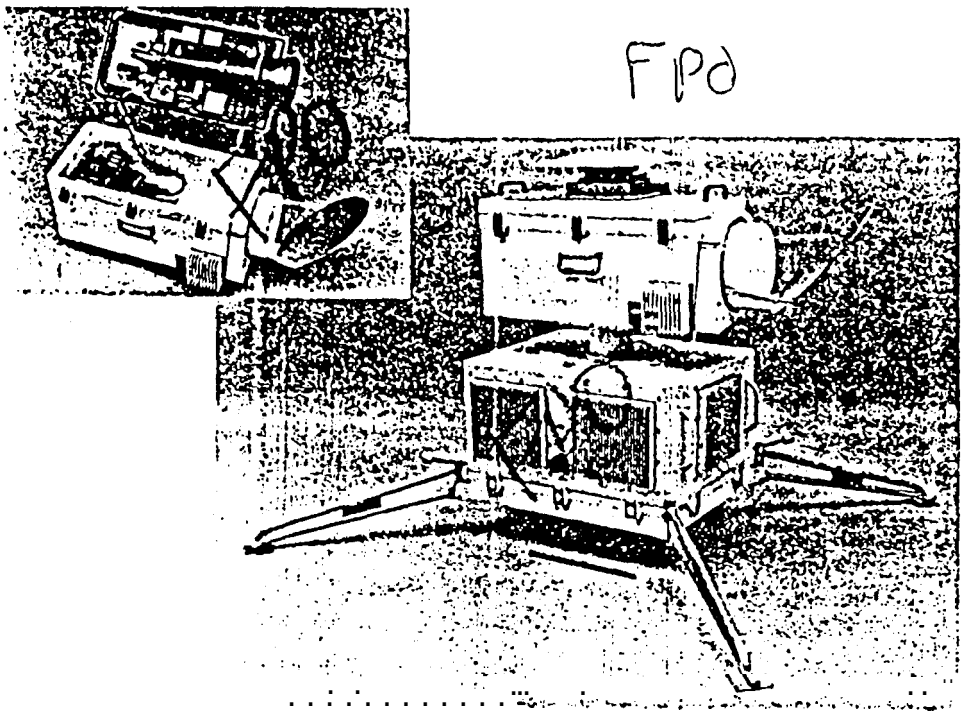

Figure 1.17. A ground-based water-vapor radiometer (WVR). The radiometer has channels at 20.7, 22.2. and 31.4 GHz, and is contained in the upper enclosure. which is shown opened in the inset. The diagonal. flat reflector at the front of this enclosure directs the sky emission into a wide bandwidth corrugated scalar feedhorn, which diplexes this signal into two independent heterodyne radiometers. One radiometer has two local oscillators that are turned on one at a time to provide the-20.7- and 22.2-GHz channels. A 1-foot ruler is shown beneath the instrument.

These cannot be resolved by even the largest single-antenna telescopes, even though much useful information can be gained by disk-averaged measurements (see Chapters 9 and 10). Arrays of antennas can be used to synthesize large virtual apertures. For example, the Very Large Array (VLA) in New Mexico (Figure 1. 19) can achieve arc-second resolution or better at several centimeter wavelengths.

The microwave sections of radiometers currently used for remote sensing are constructed from discrete components plumbed together with waveguide. The physical bulk and complexity of microwave circuits built in this way have been limiting factors in the development of many applications. For example, it has been difficult to place microwave instruments on deep-space planetary missions because of the severe weight and power constraints associated with such missions. Also, practical applications such as the ground-based mapping of tropospheric temperature and water content for weather-related purposes require networks of sensors. and are limited by the presently large costs of individual units. However, the wave

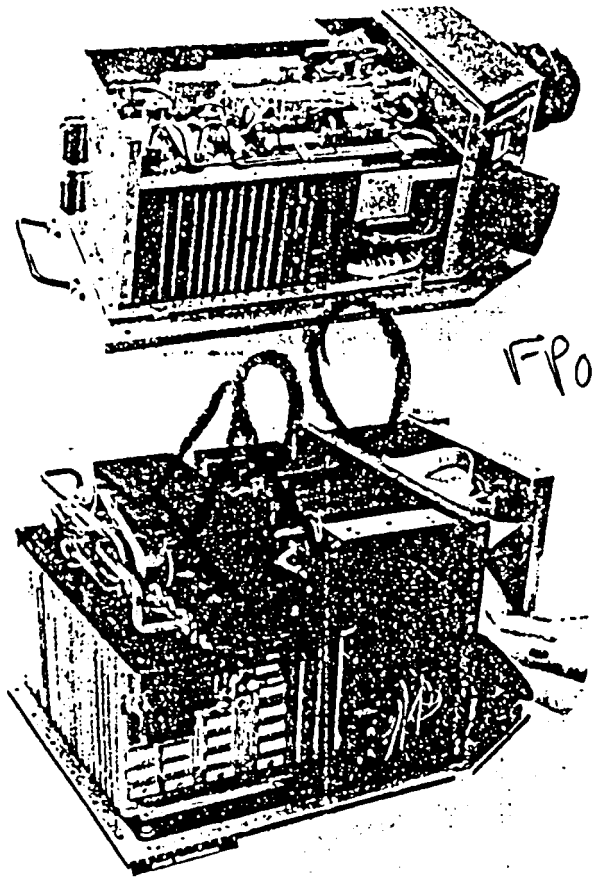

Figure 1.18. The Special Sensor Microwave Temperature SSM/T-1 (lower) and SSM/T-2 (upper) sounders. SSM/T instruments have been launched from 1979 to 1991 as part of the Defense Meteorological Satellite Program (DMSP). The SSM/T-1 has several channels in the strong oxygen band centered around 60 GHz and is used for temperature sounding. The SSM/T-2 instrument is the first of a new class of water-vapr profilers that sound the atmosphere at several frequencies in the vicinity of the strong 183-GHz H_2O line.

of miniaturization that began with the introduction of the transistor is just now beginning to reach the centimeter to millimeter microwave region. The state of the art of radiometry at frequencies up to about 100 GHz is consequently entering a slate of transition in which it can be expected that *monolithic microwave integrated circuit* (*MMIC*) components will replace many of those based on waveguide geometries. As an example. Figure 1.20 shows a prototype 30-GHz radiometer recently built at the Jet Propulsion Laboratory using only MMIC components and configured as a complete end-to-end system [41]. It is possible to construct such

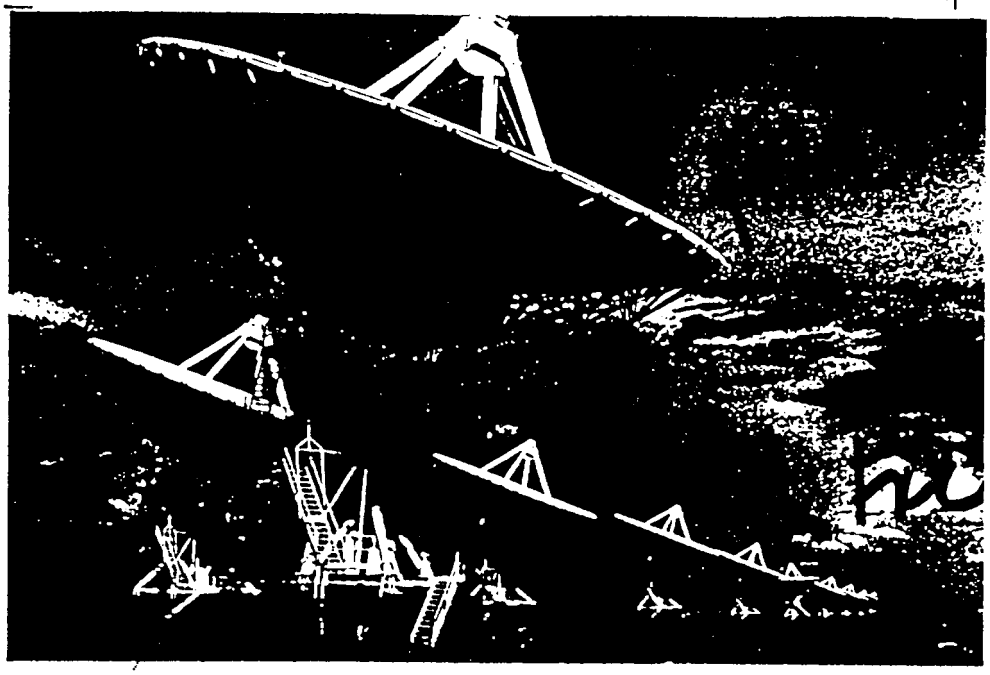

Figure 1.19. **A view of the Very Large Arr-y on the Plains of San Augustin in New Mexico.** The VLA was constructed by the National Radio Astronomical Observatory and consists of 27 antennas of 25-m diameter each, which are movable along three 20-km tracks arranged **in a "'Y'" configuration.** The array is capable of synthesizing a virtual aperture as large as 36 km **in diameter. Each antenna contains receivers at discrete wavelengths in the range 1.35-20 cm.**

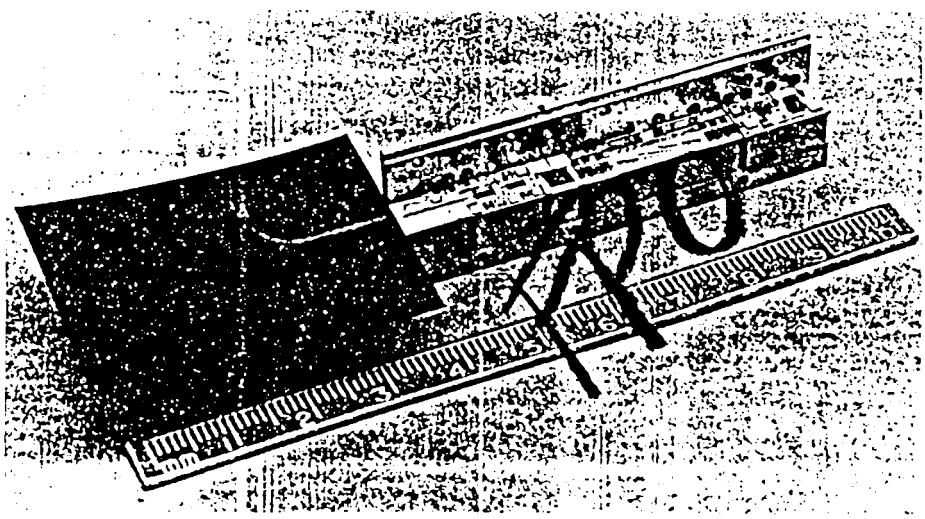

Figure 1.20. A microwave radiometer built from MMIC components. The circuit is a total power heterodyne radiometer with RF preamplification, and includes a noise source for calibration and voltage-to-frequency conversion of the radiometer output. Thermoelectric junctions (not shown) are mounted to the base to provide temperature control.

a radiometer on a single substrate, which will lead to further miniaturization and cost reduction. When this technology matures, we can expect the costs of radiometers to fall dramatically at frequencies well into the millimeter region, and many of the applications described in this volume will open up for considerable future development.

REFERENCES

1. S. Chandrasekhar, *Radiative Transfer.* Dover, New York, 1960.
2. J. D. Krause. *Radio Astronomy.* McGraw-Hill, New York. 1966.
3. L. Tsang, J. A. Kong, and R. T. Shin. *Theory of Microwave Remote Sensing.* Wiley, New York. 1985.
4. F. T. Ulaby, R. K. Moore, and A. K. Fung, *Microwave Remote Sensing: Active and Passive.* Vol. 1. Addison-Wesley, Reading, Massachusetts, 1981.
5. G. B. Rybicki and A. P. Lightman, *Radiative Processes in Astrophysics.* Wiley, New York, 1979.
6. W. V. Levitt, *Linear Integral Equations.* Dover, New York, 1950.
7. S. Twomey. *Introduction to the Mathematics of Inversion in Remote Sensing and Indirect Measurements.* Elsevier, New York, 1977.
8. F. Jay, ed., *IEEE Standard Dictionary of Electrical and Electronics Terms,* IEEE Press, New York, 1983.
9. P. W. Kruse, L. D. McGlauchlin, and R. B. McQuistan, *Elements of infrared Technology: Generation, Transmission, and Detection.* Wiley, New York, 1962.
10. M. Harwitt, *Astrophysical Concepts.* Wiley, New York, 1973.
11. H. P. Gush. M. Halpern, and E. H. Wishnow, Rocket measurement of the cosmic background radiation mm-wave spectrum. *Phys. Rev. Lett.* 6S, 537-540 (1990).
12. B. R. Bean and E. J. Dutton, *Radio Meteorology.* Dover, New York, 1968.
13. G. Evans and C. W. McLeish, *RF Radiometer Handbook.* Artech House, Dedham, Massachusetts, 1977.
14. P. F. Goldsmith. cd.. *Instrumentation and Techniques for Radio Astronomy.* IEEE Press, New York, 1988.
15. R. M. Price, Radiometer fundamentals. In *Methods of Experimental Physics.* M. L. Meeks, cd., Academic Press, New York, 1976, pp. 201-224.
16. V. Manassewitsch, *Frequency Synthesizers, Theory and Design. Wiley, New* York, 1976.
17. H. Nyquist, Thermal agitation of electric charge in conductors. *Phys. Rev.* 32, 110-113(1928).
18. C. T. Stelzreid, Microwave thermal noise standards. *IEEE Trans. Microwave Theory Tech.* MTT-16 *(9), 646-665 (1968).*
19. C. A. Balanis, *Antenna Theory Analysis and Design.* Harper & Row, New York, 1982.
20. J. D. Krause, *Antennas,* 2nd cd. McGraw-Hill, New York. 1988.
21. A. W. Love, cd., *Reflector Antennas.* IEEE Press. New York, 1988.

22. W. L. Stutzman and G. A. Thiele, *Antenna Design and Theory*. Wiley, New York, 1981.

23. Y. Rahmat-Samii and G. K. Noreen. Spacecraft antennas. In *Deep Space Telecommunications Systems Engineering* (J. H. Yuen, cd.), JPL PuM. 82-76. Jet Propulsion Laboratory, California Institute of Technology, Pasadena, 1982, pp. 413-460.

24. A. R. Thompson. J. M. Morun, and G. W. Swenson, Jr.. *Interferometry and Synthesis in Radio Astronomy*. Wiley. New York, 1986.

25. C. s. Ruf, C. T. Swift, A. B. Tanner. and D. M. Le Vine, Interferometric synthetic aperture microwave radiometry for the remote sensing of the Earth. *IEEE Trans. Geosci. Remote Sens. GE-26(5), 597-611 (1988).*

26. A. B. Tanner, Aperture synthesis for passive microwave remote sensing: The electronically steered thinned army radiometer. Ph.D. dissertation, Department of Electrical and Computer Engineering. University of Massachusetts, Amherst, 1990.

27. C. S. Ruf. Antenna performance for a synthetic aperture microwave radiometer in geosynchronous Earth orbit. In *Proceedings of the 1990 International Geoscience and Remote Sensing Symposium*, Vol. *2*, pp. 1589-1592. IEEE Press. New York, 1990.

28. R. Pettai, *Noise in Receiving Systems.* Wiley, New York, 1984.

29. P. Horowitz. J. Forster, and I. R. Linscott, The 8-million channel narrowband analyzer. In The *Search for Extraterrestrial Life: Recent Developments* (M. D. Papagiannis, cd.), IAU Symp. No. 112, pp. 361-371, Reidel Publ., Dordrecht, The Netherlands, 1985.

30. R. E. Collin, *Foundations for Microwave Engineering.* McGraw-Hill, New York, 1966.

31. S. Y. Liao, *Microwave Devices and Circuits.* Prentice-Hall, Englewood Cliffs, New Jersey, 1980.

32. J. B. Gunn, Microwave oscillations of current in III-V semiconductor. *Solid State Commun.* 1, 88-91 (1963).

33. S. M. Petty and D. L. Trowbridge, Low-noise amplifiers. In *Deep Space Network—Radio Communications Instrument for Deep Space Exploration.* JPL Publ. 82-104. Jet Propulsion Laboratory, California Institute of Technology, Pasadena, 1983.

34. M. W. Pospieszalski, S. Weinreb, R. D. Norrod, and R. Harris. FET's and HEMT's at cryogenic temperatures-their properties and use in low-noise amplifiers. *IEEE Trans. Microwave Theory Tech.* MTT-36, 552-560 (1988).

35. S. Weinreb, M. W. Pospieszalski, and R. D. Norrod, Cryogenic, HEMT, low-noise receivers for 1.3 to 43 GHz range. *IEEE MTT-S Int. Microwave Symp. Dig.* pp. 945-948 (1988).

36. P. F. Goldsmith, Quasi-optical techniques at millimeter and submillimeter wavelengths. In *Infrared and Millimeter Waves* (K. J. Button, cd.), Vol. 6. Academic Press, Ncw York, 1982.

37. F. T. Ulaby, G. I. Haddad, and C. Kukkonen, eds., *Microwave and Optical Technology Letters*, Special Issue on Terahertz Technology. Vol. 4 (1991).

38. H. Nctt and B. J. Clifton. Characteristics of a Schottky-barrier diode mixer with conical horn antenna for submillimeter wavelengths. *Int. J. Infrared Millimeter Waves* 11(11). 1333-1343 (1990).

39. A. R. Kerr and S. K. Pan. Some recent developments in the design of S1S mixers. *Int. J. Infrared Millimeter Waves* 11(10), 11 *69-II* 87 (1990).

40. M. A. Janssen, A new instrument for the determination of radio path delay due to atmospheric water vapor. *IEEE Trans. Geosci. Remote Sens. GE-23(4).* 485–490 (1985).

41. L. M. Sukamto, M. A. Janssen, and G. S. Parks, Monolithic microwave integrated circuit water vapor radiometer. In *Proceedings of the Third Specialist Meeting on Microwave Radiometry and Remote Sensing Applications, Boulder, Colorado* (E. Westwater, ed.). U.S. Govt. Printing Office, Washington, D. C., 1992 ~~(in press)~~.